Outage Performance Analysis of Non-Orthogonal Multiple Access with Time-Switching Energy Harvesting

Hoang Thien Van[1], Hoang-Sy Nguyen[2,3], Thanh-Sang Nguyen[2], Van Van Huynh[4], Thanh-Long Nguyen[2,5], Lukas Sevcik[2], Miroslav Voznak[2]
[1]*Faculty of Information Technology, Ho Chi Minh City University of Technology (HUTECH), Ho Chi Minh City, Vietnam*
[2]*IT4Innovations, VSB - Technical University of Ostrava, 17. listopadu 2172/15, Ostrava 708 00, Czech Republic*
[3]*Faculty of Information Technology, Robotics and Artificial Intelligence, Binh Duong University, Thu Dau Mot City, Binh Duong Province, Vietnam*
[4]*Modeling Evolutionary Algorithms Simulation and Artificial Intelligence, Faculty of Electrical & Electronics Engineering, Ton Duc Thang University, Ho Chi Minh City, Vietnam*
[5]*Center for Information Technology, Ho Chi Minh City University of Food Industry, Ho Chi Minh City, Vietnam*
huynhvanvan@tdtu.edu.vn

***Abstract*—In recent years, although non-orthogonal multiple access (NOMA) has shown its potentials thanks to its ability to enhance the performance of future wireless communication networks, a number of issues emerge related to the improvement of NOMA systems. In this work, we consider a half-duplex (HD) relaying cooperative NOMA network using decode-and-forward (DF) transmission mode with energy harvesting (EH) capacity, where we assume the NOMA destination (D) is able to receive two data symbols in two continuous time slots which leads to the higher transmission rate than traditional relaying networks. To analyse EH, we deploy time-switching (TS) architecture to comprehensively study the optimal transmission time and outage performance at D. In particular, we are going to obtain closed-form expressions for outage probability (OP) with optimal TS ratio for both data symbols with both exact and approximate forms. The given simulation results show that the placement of the relay (R) plays an important role in the system performance.**

***Index Terms*—Non-orthogonal multiple access; Energy harvesting; Time switching; Outage probability.**

I. Introduction

Recently, thanks to the significant rise in the number of mobile devices and the advancement of wireless technologies, they lead to the sustainable demand for better connection [1]. As a result, much research interest has been attracted by fifth-generation (5G) networks because of data transfer and services from fourth generation (4G) networks. Thus, this advancement contributes to the information access at anytime and anywhere with more applications and mobile services [2]–[4].

In order to responding to the aforementioned demands, non-orthogonal multiple access (NOMA) has attracted much attention due to its ability to deal with massive connectivity, high latency, low throughput, and low reliability [5]. In particular, multiple users in NOMA systems can be served in a time slot, spreading code, or subcarrier [6]. However, NOMA is still in the beginning stage, and more works need to be done to pave the ways for future deployments.

Despite the advantages of using NOMA in future wireless systems, it also encounters some problems, such as the short lifetime of wireless nodes. Fortunately, although that factor prevents the potentials of NOMA systems, energy harvesting (EH), which is a promising technology, can be deployed to cope with the situation [7]. In practice, energy efficiency (EE) and spectrum efficiency (SE) are key objectives in most 5G systems. Therefore, a technique so-called simultaneous wireless information power transfer (SWIPT) can help EH systems harvest energy from radio frequency (RF) signals. Based on SWIPT, time switching (TS) and power splitting (PS) are two primary EH receiver architectures deployed at the relay node. In particular, thanks to time switching (TS) and power splitting (PS) protocols, the literature in [8] came up with two new relaying networks so-called time switching-based relaying (TSR) protocol and power splitting-based relaying (PSR) protocol to support EH and information processing at the relay node. In [9], the performance of relay selection (RS) schemes in networks with multiple relays was considered. In [10], the work

Manuscript received 17 September, 2018; accepted 19 January, 2019.
This work was supported by The Ministry of Education, Youth and Sports from the Large Infrastructures for Research, Experimental Development and Innovations project "IT4Innovations National Supercomputing Center – LM2015070" and partially received a financial support from grant No. SGS SP2019/41 conducted at VSB - Technical University of Ostrava, Czech Republic.

designed a SWIPT NOMA network, where PS protocol is used with a strong channel condition, while NOMA with fixed power allocation and cognitive radio inspired NOMA with SWIPT were examined in [11].

In principle, NOMA allocates different powers to multiple users [12]–[15]. In [12], the study studied a full-duplex (FD) cooperative relaying NOMA (CR-NOMA) network, where a FD relay assists the communication between users with weak channel conditions. Meanwhile, the authors in [13] focused on a CR-NOMA adopting RS, and power allocation problems for half-duplex (HD) and FD in CR-NOMA systems were investigated in [14] to optimize the achievable data rate. In addition, the outage performance for CR-NOMA networks was considered in [15], in which closed-form expressions for outage probability were obtained.

Motivated from the aforementioned works, we design a CR-NOMA to improve the system performance. The contributions of the paper are summarized as follows:

– In this proposed NOMA system, we consider EH and information transmission (IT) time are important directly affect the system performance. Thus, we are going to optimize the IT time to drastically improve the system transmission rate.

– Next, we are going to obtain closed-form expressions for outage probability (OP) in exact and approximate forms to explore the advantages of NOMA.

– Lastly, simulation results are given to examine the impact of relay's placement, and we try to prove that the system performance in case of using NOMA outperforms traditional cooperative relaying networks (CRNs).

We divide this work into five sections. In particular, we present the system model in Section II. In Section III, we obtain the optimal IT time and closed-form expressions for the OP. In Section IV, simulation results are given. Lastly, Section V concludes the paper.

Notation: We denote the received signal-to-noise ratio (SNR) as Γ. Pr(.) stands for the probability distribution. $\mathbb{E}\{|.|\}$ represents the expectation operator. The cumulative distribution function (CDF) and probability density function (PDF) of the random variable (RV) as $F_A(x)=1-\frac{1}{\Omega_A}e^{-\frac{x}{\Omega_A}}$ and $f_A(x)=\frac{1}{\Omega_A}e^{-\frac{x}{\Omega_A}}$, where Ω_A is the average power.

II. System Model

In Fig. 1 we design a cooperative relaying network with non-orthogonal multiple access (CR-NOMA) which consists of a base station (BS) communicating with a NOMA destination (D) with the assistance of a half-duplex (HD) fixed decode-and-forward (DF) relay (R), it decodes the source data signal in one block and forward that signal in the following block to the destination node. Simultaneously, R cannot transmit and receive a data signal in HD mode. Interestingly, there is a direct connection between BS and D. Besides, R is deployed with strong channel conditions to assist D with worse channel conditions.

The addictive white Gaussian noise (AWGN) is assumed to have a negative impact on every node with zero mean n_0 and variance N_0. In addition, $g=d_Y/d_X$ is the distance ratio from $BS\to R$ and from $R\to D$. It is noted that the distance between BS and D is d_Z, so we have:

$$\begin{cases} d_X=\dfrac{d_Z}{1+g}, \\ d_Y=\dfrac{gd_Z}{1+g}. \end{cases} \quad (1)$$

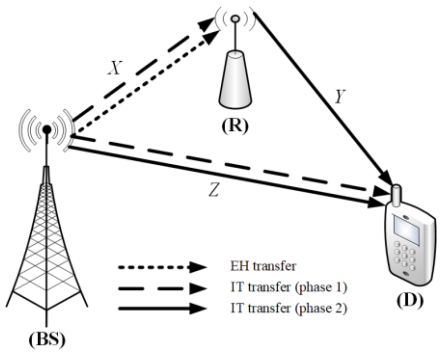

Fig. 1. System model.

Time-switching protocol: In order to study EH, we use time-switching (TS) receiver architecture at R in Fig. 2. Specifically, T is denoted as the time block for a whole communication phase, in which $(T-\delta T)$ is referred to how much energy is harvested at R while δT belongs to information transmission (IT) with half of that, $\delta/2$ utilized for the link between BS and R, and the remaining part for the link between R and D. We define $\delta\in(0,1)$ as TS ratio. In the following sections, we are going to apply TS protocol in evaluating other system performance metrics.

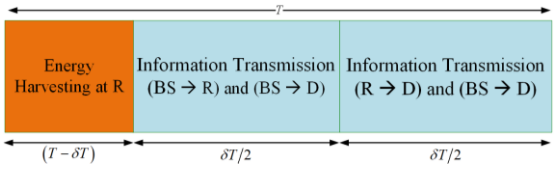

Fig. 2. Energy harvesting and information transmission protocol.

Fading channels: This system consists of two consecutive time slots in the transmission process. In particular, BS transmits a data symbol denoted as x_1 to R and D in the first time slot with $\mathbb{E}\left(|x_1|^2\right)=1$, in which BS uses the transmit power, P_S. Unlike the transmission in the first phase, we deploy power allocation at BS as a NOMA principle to differentiate two data symbols in the second time slot thanks to the characteristic of NOMA transceivers. In particular, BS forwards another data symbol, x_2 defined as $\mathbb{E}\left(|x_2|^2\right)=1$ to D with P_S, while R transmits x_1 with the transmit power at R, P_R to D. Channel coefficients of the links between BS to R, R to D, and BS are presented by D X, Y, and Z, respectively. All channels are assumed to suffer from independent and identically distributed (i.i.d) quasi-static

Rayleigh fading channel, so the channel power gain, $|A|^2$ with $A \in \{X, Y, Z\}$ follows an exponential distribution with mean value, Ω_A. The path-loss exponent is m.

A. The First Time Slot's Transmission Process

We start by expressing the amount of signal received, x_1 at both R and D as

$$y_{R,1,x_1} = \sqrt{\frac{P_S}{d_X^m}} X x_1 + n_0, \tag{2}$$

and

$$y_{D,1,x_1} = \sqrt{\frac{P_S}{d_Z^m}} Z x_1 + n_0. \tag{3}$$

Then, the harvested energy, E_h at R during $(1-\delta)T$ is given by

$$E_h = \eta P_S \frac{|X|^2}{d_X^m}(1-\delta)T, \tag{4}$$

where the energy conversion efficiency is defined as $0 < \eta < 1$.

Because BS transmits the decoded signal using E_h during $\delta T/2$, we define the transmit power at R as

$$P_R = \frac{2E_h}{\delta T} = \alpha P_S \frac{|X|^2}{d_X^m}, \tag{5}$$

where $\alpha = \dfrac{2\eta(1-\delta)}{\delta}$.

B. The Second Time Slot's Transmission Process

Likewise, the received signal at D is basically presented as

$$y_{D,2} = \sqrt{\frac{P_R}{d_Y^m}} Y x_1 + \sqrt{\frac{P_S}{d_Z^m}} Z x_2 + n_0. \tag{6}$$

Next, we compute D's received signal by replacing the obtained expression for P_R from (5) into (6) as

$$y_{D,2} = \sqrt{\alpha \frac{P_S}{d_Y^m} \frac{|X|^2}{d_X^m}} Y x_1 + \sqrt{\frac{P_S}{d_Z^m}} Z x_2 + n_0. \tag{7}$$

III. PERFORMANCE ANALYSIS

In this part, we are going to optimize the IT time to achieve the optimal maximum transmission rate and obtain closed-form expressions for the outage probability (OP). Therefore, we now start with the received signal-to-noise ratio (SNR).

A. The Received Signal-to-Noise Ratio (SNR)

We define the received SNR as $\Gamma = \mathbb{E}\{|\text{signal}|^2\} / \mathbb{E}\{|\text{overallnoise}|^2\}$. Thus, based on (2) and (3), the SNRs for, x_1 at R and D is expressed by

$$\Gamma_{R,1,x_1} = \beta \frac{|X|^2}{d_X^m}, \tag{8}$$

and

$$\Gamma_{D,1,x_1} = \beta \frac{|Z|^2}{d_Z^m}, \tag{9}$$

where the transmit SNR of BS is represented by $\beta = \dfrac{P_S}{N_0}$.

For simplicity, we decided to take advantage of successive interference cancellation (SIC) our system. In principle, D decodes x_1 by treating x_2 as a noise term which is later eliminated from $y_{D,2}$ to decode x_2. Consequently, we derive the received SNRs at D for x_1 and x_2 as

$$\Gamma_{D,2,x_1} = \frac{\alpha\beta \dfrac{|X|^2}{d_X^m} \dfrac{|Y|^2}{d_Y^m}}{\beta \dfrac{|Z|^2}{d_Z^m} + 1}, \tag{10}$$

and

$$\Gamma_{D,2,x_2} = \beta \frac{|Z|^2}{d_Z^m}. \tag{11}$$

Hence, we compute the end-to-end achievable data rate at D for x_1 and both x_1 and x_2 over the $\delta/2$ time slot as

$$R_{e2e,x_1} = \frac{\delta}{2} \log_2\left(1 + \Gamma_{e2e,x_1}\right), \tag{12}$$

and

$$R_{D,1,x_1} = R_{D,2,x_2} = \frac{\delta}{2} \log_2\left(1 + \Gamma_{D,1,x_1}\right), \tag{13}$$

where $\Gamma_{e2e,x_1} = \min\{\Gamma_{R,1,x_1}, \Gamma_{D,2,x_1}\}$ thanks to the deployment of fixed DF at the transceiver.

B. The Optimization of Information Transmission Time

In practice, the transmission rate is a function of δ of the end-to-end SNR. In this part, we are going to optimize the IT time, δ^* to achieve the maximum transmission rate in (12) with $\delta \in (0,1)$.

Due to the changes of the power level at R, the optimization of δ can be achieved by

$$\delta^* = \text{argmax}\,\Gamma_{e2e,x_1} = \text{argmax}\,\min\left(\Gamma_{R,1,x_1}, \Gamma_{D,2,x_1}\right), \quad (14)$$

where subject to $\delta \in (0,1)$.

As a result, the optimal TS δ^* is equivalent to the following

$$\Gamma_{R,1,x_1} = \Gamma_{D,2,x_1}. \quad (15)$$

In this work, because of the availability of the channel state information (CSI) at solely D. Base on (8) and (10), we can express the average optimal IT time after some manipulations as

$$\delta^* = \left[\frac{\beta\Omega_Z d_Y^m}{2\eta\Omega_Y d_Z^m} + \frac{d_Y^m}{2\eta\Omega_Y} + 1\right]^{-1}. \quad (16)$$

Remark 1: The fading gain, Z of the $BS \to D$ link is small than Y of the $R \to D$ link due to the changes in distance. In addition, the stronger the $BS \to R$ link becomes, the shorter the distance between BS and R is and shorter time required by R during $(1-\delta)$ to harvest more energy. This contributes to better the transmission rate.

C. Outage Performance of NOMA

In practice, OP is the probability that the information rate is less than the required threshold information rate, Γ_0 which is defined as $OP = \Pr(\Gamma < \Gamma_0) = F_\Gamma(\Gamma_0)$. Besides, the threshold $\Gamma_0 = 2^{2R_0} - 1$ is related to the target rate R_0 in HD mode. Thus, we have to evaluate the CDF first on the *Proposition* 1 before deriving OP later on.

Proposition 1. In this CR-NOMA, we compute the OPs, OP_{x_1} and OP_{x_2} for x_1 and x_2 respectively as

$$OP_{x_1} = \left(1 - e^{-\upsilon_1}\right)\left(1 - \frac{1}{\Omega_Z}\int_{x=0}^{\infty} e^{-\frac{x}{\Omega_Z} - \upsilon_2}\,\Upsilon dx\right), \quad (17)$$

and

$$OP_{x_2} = 1 - \frac{1}{\Omega_Z} e^{-\upsilon_1}\int_{x=0}^{\infty} e^{-\frac{z}{\Omega_Z}}\,\Upsilon dx, \quad (18)$$

where $\upsilon_1 = \dfrac{\Gamma_0 d_Z^m}{\beta\Omega_Z}$, $\upsilon_2 = \dfrac{\Gamma_0 d_X^m}{\beta\Omega_X}$, and $\Upsilon = \sqrt{\dfrac{4\Gamma_0\left(\beta d_Z^{-m} x + 1\right) d_X^m d_Y^m}{\alpha\beta\Omega_X\Omega_Y}} \times K_1\left(\sqrt{\dfrac{4\Gamma_0\left(\beta d_Z^{-m} x + 1\right) d_X^m d_Y^m}{\alpha\beta\Omega_X\Omega_Y}}\right)$.

Proof:

with the CDF for $\Gamma_{R,1,x_1}$ and $\Gamma_{D,1,x_1}$, we have

$$F_{\Gamma_{R,1,x_1}}(\Gamma_0) = 1 - e^{-\frac{\Gamma_0 d_X^m}{\beta\Omega_X}}, \quad (19)$$

and

$$F_{\Gamma_{D,1,x_1}}(\Gamma_0) = 1 - e^{-\frac{\Gamma_0 d_Z^m}{\beta\Omega_Z}}. \quad (20)$$

As mentioned, the CDF of $\Gamma_{D,2,x_1}$ should be evaluated first before the OP at D for x_1 is achieved. Thus, $F_{\Gamma_{D,2,x_1}}(\Gamma_0)$ is conditioned on $|Z|^2$ by

$$F_{\Gamma_{D,2,x_1}}(\Gamma_0) = \Pr\left(|X|^2 \le \frac{\Gamma_0\left(\beta\dfrac{|Z|^2}{d_Z^m} + 1\right)}{\alpha\beta\dfrac{|Y|^2}{d_X^m d_Y^m}}\right) =$$

$$= \frac{1}{\Omega_Y}\int_0^{\infty}\left(1 - e^{-\frac{1}{y}\left(\frac{\Gamma_0\left(\beta\frac{|Z|^2}{d_Z^m}+1\right)}{\alpha\beta\frac{\Omega_X}{d_X^m d_Y^m}}\right)}\right) e^{-\frac{y}{\Omega_Y}} dy =$$

$$= 1 - \sqrt{\frac{4\Gamma_0\left(\beta\dfrac{|Z|^2}{d_Z^m} + 1\right)}{\alpha\beta\dfrac{\Omega_X\Omega_Y}{d_X^m d_Y^m}}} K_1\left(\sqrt{\frac{4\Gamma_0\left(\beta\dfrac{|Z|^2}{d_Z^m} + 1\right)}{\alpha\beta\dfrac{\Omega_X\Omega_Y}{d_X^m d_Y^m}}}\right), \quad (21)$$

where the desired expression is obtained following from $\int_0^{\infty} e^{-\frac{\beta}{4x} - \gamma x} dx = \sqrt{\frac{\beta}{\gamma}} K_1\left(\sqrt{\beta\gamma}\right)$ in [16, eq.(3.324.1)].

Therefore, we rewrite the CDF of $\Gamma_{D,2,x_1}$ over $|Z|^2$ by

$$F_{\Gamma_{D,2,x_1}}(\Gamma_0) = 1 - \frac{1}{\Omega_Z} \times$$

$$\times \int_0^{\infty}\left(e^{-\frac{x}{\Omega_Z}} \sqrt{\frac{4\Gamma_0\left(\beta\dfrac{x}{d_Z^m} + 1\right)}{\alpha\beta\dfrac{\Omega_X\Omega_Y}{d_X^m d_Y^m}}} K_1\left(\sqrt{\frac{4\Gamma_0\left(\beta\dfrac{x}{d_Z^m} + 1\right)}{\alpha\beta\dfrac{\Omega_X\Omega_Y}{d_X^m d_Y^m}}}\right)\right) dx. \quad (22)$$

If x_1 cannot be decoded by one of the links, an outage event may happen. However, using (19) and (24), the end-to-end SNR OP at D is written as

$$OP_{e2e,x_1} \triangleq F_{\Gamma_{R,1,x_1}}(\Gamma_0) + F_{\Gamma_{D,2,x_1}}(\Gamma_0) -$$

$$-F_{\Gamma_{R,1,x_1}}(\Gamma_0) \times F_{\Gamma_{D,2,x_1}}(\Gamma_0) \triangleq 1 - \frac{1}{\Omega_Z} \times$$

$$\times\int_{x=0}^{\infty} e^{-\frac{x}{\Omega_Z}-\frac{\Gamma_0 d_X^m}{\beta\Omega_X}} \sqrt{\frac{4\Gamma_0\left(\beta d_Z^{-m}x+1\right)}{\alpha\beta d_X^{-m}d_Y^{-m}\Omega_X\Omega_Y}}\times$$
$$\times K_1\left(\sqrt{\frac{4\Gamma_0\left(\beta d_Z^{-m}x+1\right)}{\alpha\beta d_X^{-m}d_Y^{-m}\Omega_X\Omega_Y}}\right)dx. \quad (23)$$

Interestingly, the total value of OP of x_1 is computed by using selection combining technique at R as

$$OP_{x_1} = F_{\Gamma_{D,1,x_1}}\left(\Gamma_0\right)\times OP_{\Gamma_{e2e,x_1}}\left(\Gamma_0\right). \quad (24)$$

Replacing (20) and (23) into (24), (17) is obtained.

Furthermore, we achieve the OP of x_2 in the BS-D link, OP_{x_2} as

$$OP_{x_2} = 1-\Pr\left(\Gamma_{D,2,x_1}>\Gamma_0,\Gamma_{D,2,x_2}>\Gamma_0\right)=$$
$$=1-\left(1-F_{\Gamma_{D,2,x_1}}(\Gamma_0)\right)\times\left(1-F_{\Gamma_{D,2,x_2}}(\Gamma_0)\right), \quad (25)$$

where $F_{\Gamma_{D,2,x_1}}\left(\Gamma_0\right)=1-e^{-\frac{\Gamma_0 d_Z^m}{\beta\Omega_Z}}$. Therefore, we derive the result following from (18).

This ends the proof for *Proposition* 1.

We see that although it is not easy to achieve a closed-form expression in *Proposition* 1, we are going to express it in *Proposition* 2 due to using the integral item to reduce the computation complexity.

Proposition 2. In the asymptotic high SNR regime, we can easily approximate the result of *Proposition* 1 as

$$OP_{x_1}^{\infty}\approx\left(1-e^{-\upsilon_1}\right)\left(1-\frac{1}{\Omega_Z}\int_{x=0}^{\infty}e^{-\frac{x}{\Omega_Z}-\upsilon_2}\Upsilon^{\infty}dx\right), \quad (26)$$

and

$$OP_{x_2}^{\infty}\approx 1-\frac{1}{\Omega_Z}e^{-\upsilon_1}\int_{x=0}^{\infty}e^{-\frac{x}{\Omega_Z}}\Upsilon^{\infty}dx, \quad (27)$$

where $\Upsilon^{\infty}=\sqrt{\frac{4\Gamma_0 d_Z^{-m}d_X^m d_Y^m x}{\alpha\Omega_X\Omega_Y}}K_1\left(\sqrt{\frac{4\Gamma_0 d_Z^{-m}d_X^m d_Y^m x}{\alpha\Omega_X\Omega_Y}}\right)$.

Proof:

Due to conducting the similar steps for the proof in *Proposition* 1, we upper bound the modified Bessel function of the second kind as $xK_1(x)\to 1$, when $x\to 0$. Therefore, $\beta\to\infty$, the CDF in (22) can be expressed at high SNR as

$$F_{\Gamma_{D,2,x_1}}(\Gamma_0)=$$
$$=1-\frac{1}{\Omega_Z}\int_{x=0}^{\infty}e^{-\frac{x}{\Omega_Z}}\sqrt{\frac{4\Gamma_0\left(\beta d_Z^{-m}x+1\right)}{\alpha\beta d_X^{-m}d_Y^{-m}\Omega_X\Omega_Y}}\times$$
$$\times K_1\left(\sqrt{\frac{4\Gamma_0\left(\beta d_Z^{-m}x+1\right)}{\alpha\beta d_X^{-m}d_Y^{-m}\Omega_X\Omega_Y}}\right)dx\le$$
$$\le 1-\frac{1}{\Omega_Z}\int_{x=0}^{\infty}e^{-\frac{x}{\Omega_Z}}\sqrt{\frac{4\Gamma_0 d_Z^{-m}x}{\alpha d_X^{-m}d_Y^{-m}\Omega_X\Omega_Y}}\times$$
$$\times K_1\left(\sqrt{\frac{4\Gamma_0 d_Z^{-m}x}{\alpha d_X^{-m}d_Y^{-m}\Omega_X\Omega_Y}}\right)dx. \quad (28)$$

Finally, we can apply the approximations of $e^{-x}=1-x$ when $x\to 0$ on (17). After some algebraic manipulations, (26) can be obtained. Similarly, the approximate outage probability for x_2 in (27) can be obtained.

This ends the proof for *Proposition* 2.

IV. NUMERICAL RESULTS

In this section, the outage performance with the optimal IT time are simulated to give better insights into the system performance. In addition, the placement of relay regarding the distance allocation in this system is also illustrated. Note that the distance allocation ratio between d_X and d_Y is assumed to be equal, $g=1$. In order to prove the robustness of the derived expressions, we compare with complementary Monte Carlo-simulated performance results. Without the loss of generality, we generate 10^6 realizations of Rayleigh distribution RVs. The simulation systems follow some parameters summarized in Table I.

In Fig. 3, the considered CR-NOMA is compared with a traditional CRN without NOMA in terms of appropriate and exact OP with both data symbols, i.e., x_1 and x_2 versus the transmit SNR, β. We can see that thanks to the principles of NOMA, data symbols, x_1 and x_2 can be decoded by using SIC technique. Both OPs decrease as the transmit SNR, β rises. In addition, our CR-NOMA is outperforms the traditional CRN with x_1 due to its ability to combine signals of CRN and limit the performance of direct communication between BS and D.

TABLE I. SIMULATION PARAMETERS.

Parameter	Value	Parameter	Value
R_0	1 (bps/Hz)	m	2.7
δ	0.7	d_Z	1
η	1	$\Omega_A, A\in\{X,Y,Z\}$	1

In Fig. 4, we depict OP with different placements of R, including Case 1 (Close to BS with 3:7 ratio), Case 2 (In the middle with 1:1 ratio), and Case 3 (Far from BS with 7:3 ratio) based on the distance allocation between BS and D. Therefore, the impact of R's location degrades the OP when R and D is close together. As a result, this restricts the system transmission rate.

In Fig. 5, the transmission rate is depicted as a function of TS ratio, δ. It is noted that we set the transmit SNR to a fixed value of 5(dB). The existing CR-NOMA outperforms

the traditional CR-OMA in terms of the transmission rate. It can be clearly seen that as TS ratio increases from 0.7 to 1, CR-OMA witnesses a significant drop in transmission rate. This phenomenon happens because SIC is deployed at D to make the transmission of data symbol possible in the second time slot. Besides that, with the assistance of R, the fading gain of data symbol can be mitigated by reducing the distance between R and D.

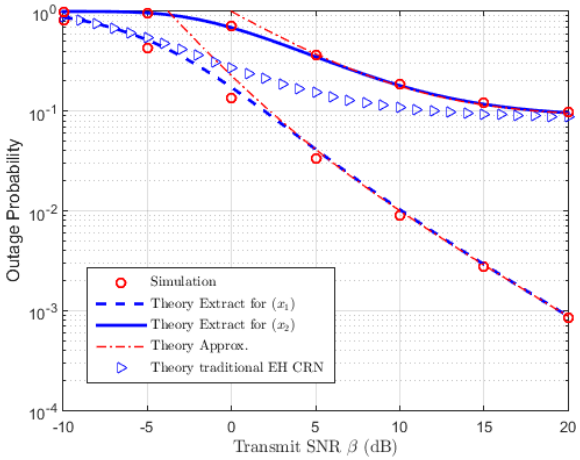

Fig. 3. Exact and approximate OP versus the transmit SNR.

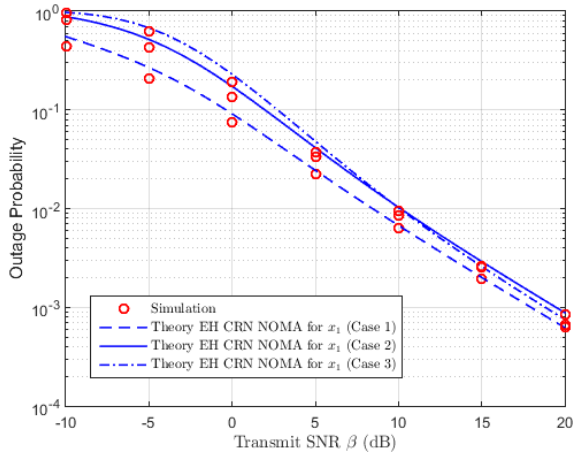

Fig. 4. OP for x_1 versus the transmit SNR.

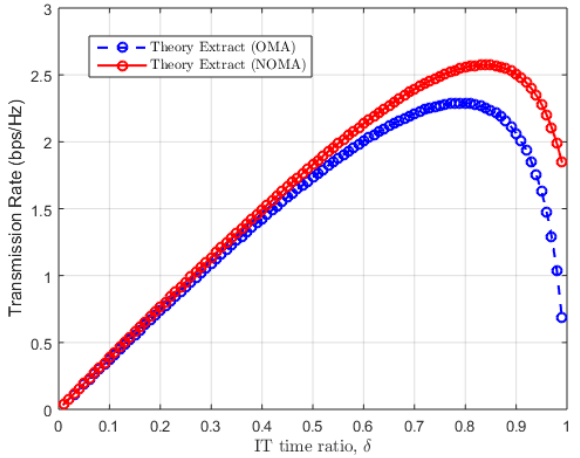

Fig. 5. OP as a function of the transmit SNR in case of optimal IT time and fixed IT time.

In Fig. 6, the OP with optimal IT time is shown as a function of the transmit SNR with the fixed IT time at $\delta = 0.7$, $d_Z = 2$, and $g = (d_X : d_Y) = (1:1)$ ratio. It is evident that the OP of D using TS protocol experiences a steady decrease as the transmit SNR increases, because the optimal IT time ensures the decoding correctness of both data symbols, x_1 and x_2 at D.

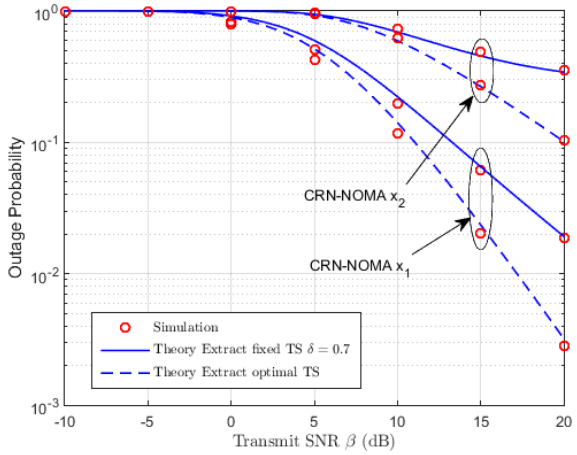

Fig. 6. OP as a function of the transmit SNR in case of optimal IT time and fixed IT time.

V. CONCLUSIONS

In this work, owning to the benefits of NOMA systems, we decided to study an EH CR-NOMA using TS receiver architecture to study EH. In particular, we obtained the optimal IT time to boost the transmission rate. Furthermore, we achieved the closed-form expressions for OP at D in exact and approximate forms. Most importantly, the proposed CR-NOMA system is superior to conventional CRNs in terms of OP in the whole SNR regime.

REFERENCES

[1] A. Gupta, R. K. Jha, "A survey of 5G network: architecture and emerging technologies", *IEEE Access*, vol. 3, pp. 1206–1232, 2015. DOI: 10.1109/ACCESS.2015.2461602.

[2] L. Zhang, M. Xiao, G. Wu, M. Alam, Y. C. Liang, S. Li, "A survey of advanced techniques for spectrum sharing in 5G networks", *IEEE Wireless Communications*, vol. 24, no. 5, pp. 44–51, 2017. DOI: 10.1109/MWC.2017.1700069.

[3] A Santamaria, M Tropea, P Fazio, F De Rango, "Managing emergency situations in VANET through heterogeneous technologies cooperation", *Sensors*, vol. 18, no. 5, pp. 1461, 2018. DOI: 10.3390/s18051461.

[4] M. Tropea, F. Veltri, F. De Rango, A.-F. Santamaria, L. Belcastro, "Two step based QoS scheduler for DVB-S2 satellite system", in *IEEE Int. Conf. Communications (ICC 2011)*, Kyoto, Japan, 2011, pp. 1–5. DOI: 10.1109/icc.2011.5963226.

[5] S. M. R. Islam, N. Avazov, O. A. Dobre, and K. Kwak, "Power-domain non-orthogonal multiple access (NOMA) in 5G systems: potentials and challenges", *IEEE Communications Surveys & Tutorials*, vol. 19, no. 2, pp. 721–742, 2017. DOI: 10.1109/COMST.2016.2621116.

[6] Y. Cai, Z. Qin, F. Cui, G. Y. Li, J. A. McCann, "Modulation and Multiple Access for 5G Networks", *IEEE Communications Surveys and Tutorials*, vol. 20, pp. 629–646, 2018. DOI: 10.1109/COMST.2017.2766698.

[7] X. Lu, P. Wang, D. Niyato, D. I. Kim, Z. Han, "Wireless networks with RF energy harvesting: a contemporary survey", *IEEE Communications Surveys and Tutorials*, vol. 17, pp. 757–789, 2015. DOI: 10.1109/COMST.2014.2368999.

[8] A. A. Nasir, X. Zhou, S. Durrani, R. A. Kenned, "Relaying protocols for wireless energy harvesting and information processing", *IEEE Trans. Wireless Communications*, vol. 12, no. 5, pp. 3622–3636, 2013. DOI: 10.1109/TWC.2013.062413.122042.

[9] H. S. Nguyen, T. S. Nguyen, V. T. Vo, M. Voznak, "Hybrid full-duplex/half-duplex relay selection scheme with optimal power under individual power constraints and energy harvesting", *Computer*

Communications, vol. 124, pp. 31–44, 2018. DOI: 10.1016/j.comcom.2018.04.014.

[10] Y. Xu, C. Shen, Z. Ding, X. Sun, S. Yan, G. Zhu, Z. Zhong, "Joint beamforming and power-splitting control in downlink cooperative SWIPT NOMA systems", *IEEE Trans. Signal Processing*, vol. 65, no. 18, pp. 4874–4886, 2017. DOI: 10.1109/TSP.2017.2715008.

[11] X. Wang, J. Wang, L. He, J. Song, "Outage analysis for downlink NOMA with statistical channel state information", *IEEE Wireless Communications Letters*, vol. 7, no. 2, pp. 142–145, 2018. DOI: 10.1109/LWC.2017.2761343.

[12] C. Zhong, Z. Zhang, "Non-orthogonal multiple access with cooperative full-duplex relaying", *IEEE Communications Letters*, vol. 20, no. 12, pp. 2478–2481, 2016. DOI: 10.1109/LCOMM.2016.2611500

[13] J. Chen, L. Yang, M. S. Alouini, "Performance analysis of cooperative NOMA schemes in spatially random relaying networks", *IEEE Access*, vol. 6, pp. 33159–33168, 2018. DOI: 10.1109/ACCESS.2018.2846773.

[14] G. Liu, X. Chen, Z. Ding, Z. Ma, F. R. Yu, "Hybrid half-duplex/full-duplex cooperative non-orthogonal multiple access with transmit power adaptation", *IEEE Trans. Wireless Communications*, vol. 17, no. 1, pp. 506–519, 2018. DOI: 10.1109/TWC.2017.2767601.

[15] W. Han, J. Ge, J. Men, "Performance analysis for NOMA energy harvesting relaying networks with transmit antenna selection and maximal-ratio combining over Nakagami-m fading", *IEEE Communications Letters*, vol. 10, no. 18, pp. 2687–2693, 2016. DOI: 10.1049/iet-com.2016.0630.

[16] I. S. Gradshtey, I. M. Ryzhik, *Table of Integrals, Series, and Products, 4th ed.* Academic Press, Inc., 1980. DOI: 10.1016/C2010-0-64839-5.